Molecular Biology of the Cell
Vol. 19, 1093–1103, March 2008

α-Synuclein–induced Aggregation of Cytoplasmic Vesicles in *Saccharomyces cerevisiae*

James H. Soper,*† Subhojit Roy,*† Anna Stieber,*† Eliza Lee,*† Robert B. Wilson,† John Q. Trojanowski,*† Christopher G. Burd,‡ and Virginia M.-Y. Lee*†

*Center for Neurodegenerative Disease Research and Departments of †Pathology and Laboratory Medicine and ‡Cell and Developmental Biology, University of Pennsylvania, Philadelphia, PA 19104

Submitted August 29, 2007; Revised December 12, 2007; Accepted December 20, 2007
Monitoring Editor: Jeffrey Brodsky

Aggregated α-synuclein (α-syn) fibrils form Lewy bodies (LBs), the signature lesions of Parkinson's disease (PD) and related synucleinopathies, but the pathogenesis and neurodegenerative effects of LBs remain enigmatic. Recent studies have shown that when overexpressed in *Saccharomyces cerevisiae*, α-syn localizes to plasma membranes and forms cytoplasmic accumulations similar to human α-syn inclusions. However, the exact nature, composition, temporal evolution, and underlying mechanisms of yeast α-syn accumulations and their relevance to human synucleinopathies are unknown. Here we provide ultrastructural evidence that α-syn accumulations are not comprised of LB-like fibrils, but are associated with clusters of vesicles. Live-cell imaging showed α-syn initially localized to the plasma membrane and subsequently formed accumulations in association with vesicles. Imaging of truncated and mutant forms of α-syn revealed the molecular determinants and vesicular trafficking pathways underlying this pathological process. Because vesicular clustering is also found in LB-containing neurons of PD brains, α-syn–mediated vesicular accumulation in yeast represents a model system to study specific aspects of neurodegeneration in PD and related synucleinopathies.

INTRODUCTION

Parkinson's disease (PD) is the most prevalent neurodegenerative movement disorder and is characterized by bradykinesia, rigidity, postural instability, and resting tremor (Galvin *et al.*, 2001; Forman *et al.*, 2005), as well as by the loss of dopaminergic neurons and presence of neuronal inclusions, known as Lewy bodies (LBs) and Lewy neurites (Forman *et al.*, 2005). The identification of an α-syn gene (*SNCA*) mutation associated with autosomal dominant PD (Polymeropoulos *et al.*, 1997), and the identification of fibrillar α-syn as the principal component of LB pathology (Spillantini *et al.*, 1997), indicate that the LBs formed by α-syn define classic PD and are implicated in disease pathogenesis. The subsequent identification of additional disease-linked *SNCA* mutations (Polymeropoulos *et al.*, 1997; Kruger *et al.*, 1998; Zarranz *et al.*, 2004), as well as replications of the *SNCA* gene (Singleton *et al.*, 2003; Chartier-Harlin *et al.*, 2004), indicate that both mutant α-syn and increased expression of wild-type (WT) α-syn can cause neurodegeneration.

In addition to PD, filamentous α-syn inclusions have been detected in other neurodegenerative diseases including the LB variant of Alzheimer's disease, dementia with LBs, neurodegeneration with brain iron accumulation type-1, and multiple system atrophy, which are collectively known as synucleinopathies (Spillantini *et al.*, 1997; Duda *et al.*, 2000). α-syn fibrils exhibit properties of amyloid (Spillantini *et al.*, 1998), and α-syn assembles into amyloid fibrils in vitro (Han *et al.*, 1995; Giasson *et al.*, 1999), whereas *SNCA* mutations can accelerate α-syn fibrillization (Conway *et al.*, 1998; Greenbaum *et al.*, 2005). Therefore, it is plausible that α-syn misfolds and aggregates into amyloid fibrils that are neurotoxic and play a causative role in the pathogenesis of PD. Thus, the elucidation of these processes could be exploited for PD drug discovery.

α-syn, a short 140-amino acid protein (Iwai *et al.*, 1995) is localized to synaptic terminals (Maroteaux and Scheller, 1991) where it appears to play a role in regulating the distal pool of presynaptic vesicles (Murphy *et al.*, 2000, Cabin *et al.*, 2002) and dopamine release (Abeliovich *et al.*, 2000) or functions as a chaperone (Chandra *et al.*, 2005). Furthermore, the N-terminus of α-syn contains several imperfect KTKEGV repeats (Maroteaux *et al.*, 1988; George *et al.*, 1995; Weinreb *et al.*, 1996), which are thought to mediate binding to membranes by interacting with phospholipids and shifting from a random coil to an α-helical conformation (Davidson *et al.*, 1998; Perrin *et al.*, 2000; Kim *et al.*, 2006). Interestingly, the PD familial mutation A30P in α-syn showed reduced binding to membranes due to the Ala→Prosubstitution in repeat 2, which disrupts membrane interaction (Jensen *et al.*, 1998; Cole *et al.*, 2002). The central region of α-syn is known as the NAC domain, and it contains hydrophobic amino acids required for fibrillization, particularly residues 71-82 (Giasson *et al.*, 2001).

Over the past 10 years, multiple in vitro, animal, and cell culture models have been developed to model LB formation and elucidate mechanisms of LB-mediated neurodegeneration. Recent studies have demonstrated that overexpressed α-syn in *Saccharomyces cerevisiae* localizes to the plasma membrane and forms inclusions (Outeiro and Lindquist,

This article was published online ahead of print in *MBC in Press* (http://www.molbiolcell.org/cgi/doi/10.1091/mbc.E07–08–0827) on January 9, 2008.

Address correspondence to: Virginia M.-Y. Lee (vmylee@mail.med.upenn.edu).

Abbreviations used: α-syn, α-synuclein; EM, electron microscopy; ER, endoplasmic reticulum; GTPase, guanosine triphosphatase; PD, Parkinson's disease; WT, wild type.

2003; Flower *et al.*, 2005). Expression of α-syn in yeast also was shown to inhibit growth, induce accumulation of lipid droplets, alter vesicle trafficking (Outeiro and Lindquist, 2003), increase reactive oxygen species (Flower *et al.*, 2005), and stimulate the heat shock response (Dixon *et al.*, 2005). Furthermore, proteins involved in endoplasmic reticulum (ER)-to-Golgi trafficking may be involved in this α-syn–induced growth defect because this defect was rescued by overexpressing Ypt1p, a Rab guanosine triphosphatase (GTPase; Cooper *et al.*, 2006). Interestingly, Ypt1p was also found to associate with the α-syn accumulations in yeast. To elucidate this pathological process, we examined the temporal sequence of α-syn accumulation in the cytoplasm of *S. cerevisiae* by following the changes in α-syn-enhanced green fluorescent protein (EGFP) localization using time-lapse microscopy. We then identified distinct structural domains of α-syn that mediate this process. Importantly, ultrastructural studies failed to detect α-syn fibrils or LB-like inclusions but instead identified the α-syn accumulations as clusters of vesicles of varying sizes. These vesicle clusters bear markers of secretory vesicles as well as ER-Golgi transport vesicles, and α-syn–induced vesicle accumulation also disrupted early and late Golgi components. Because vesicles and membranous profiles also accumulate at the periphery of LBs in PD brain, α-syn–induced vesicular clustering in the cytoplasm of *S. cerevisiae* recapitulates features of PD that may underlie mechanisms of neurodegeneration in PD.

MATERIALS AND METHODS

Yeast Strains and Media

The BY4742 (*MAT α his3Δ1 leu2Δ0 lys2Δ0 ura3Δ0*) strain of *S. cerevisiae* was used for all experiments in this study. Transformation of yeast was performed using a standard lithium polyethylene glycol transformation procedure (Gietz *et al.*, 1992). Yeast cultures were grown in selective minimal media, containing 2% glucose or 2% galactose, deficient in the required amino acids. For induction of gene expression, cells were cultured in glucose media overnight, and cells from this culture were taken to inoculate a second culture (starting A_{600} = 0.1) in galactose media, which was then grown at 30°C for 16 h.

Plasmids

Both 2μ and integrative expression systems were generated and used for experimentation. To generate full-length, truncated, or mutated α-syn as well as β-syn plasmids, primer sequences for the corresponding cDNAs were amplified from our mammalian pcDNA3.1 (Invitrogen, Carlsbad, CA) α-syn constructs. EGFP sequences were similarly amplified out of pIRES-EGFP vector (Clontech, Palo Alto, CA). These α-syn and EGFP products were sequenced and digested with KpnI/HindIII and HindIII/XhoI, respectively, and ligated into the MCS of the yeast vector, pYES2 (Invitrogen).

Integrative strains were generated by PCR amplification of the Gal1 promoter, α-syn protein sequence, transcription terminator, and selection marker sequence out of the PYES2 vector. Primer sequences were chosen for directed integration into the yeast genome 500 base pairs upstream of the Gal1 promoter. For overexpression of 3HA-Ypt1p and 3HA-Sec4p, we used the pRS413 vector.

Growth Assay

Growth was measured on solid media by making serial fivefold dilutions of log-phase cultures, starting with A_{600} = 0.4. Samples of each dilution were spotted onto minimal media glucose and galactose plates, with appropriate amino acids for selection. Plates were incubated at 30°C for 2–4 d.

Immunoblot Analysis

Cell extracts were prepared as described previously (Kushnirov, 2000). Briefly, cells were grown in galactose media to log-phase. Equal amounts of cells were pelleted by centrifugation, resuspended in 1 volume water, and treated with 1 volume 0.2 M NaOH for 10 min. Cells were pelleted again, resuspended in SDS-PAGE buffer, and boiled for 5 min, and protein samples were separated by SDS-PAGE.

Antibodies

For immunoblotting, we used LB509, an anti-α-syn mouse mAb recognizing residues 115-122 (Jakes *et al.*, 1999), Syn303, an anti-α-syn mAb that recognize an epitope containing residues 1-5 of α-syn (Duda *et al.*, 2002); MAB2510, a GFP mAb (Chemicon, Temecula, CA); Syn 207, an anti-β-syn mAb (Giasson *et al.*, 2000); MAB1864, an anti-α-tubulin antibody (Chemicon); and Ab4645, an anti-Pma1 antibody (Abcam, Cambridge, MA).

Subcellular Fractionation

Membrane fractionation was performed as previously described (Juschke *et al.*, 2004). Briefly, logarithmically growing cells were washed in 20 mM HEPES, pH 7.5, 20 mM NaF, and 20 mM NaN_3. Cells were lysed in 25 mM Tris/HCl, pH 8.0, 2.5 mM EDTA, and 0.1 mM phenylmethylsulfonyl fluoride, with protease inhibitors, by vortexing with glass beads. Unbroken cells were cleared by centrifugation at 1200 × *g* for 2 min. The lysate was then subjected to centrifugation at 25,000 × *g* for 20 min. The supernatant was retained as the cytosolic fraction, and the pellet was resuspended in 0.55 ml of 10 mM Tris/HCl, pH 7.4, 0.2 mM EDTA, 0.2 mM dithiothreitol, 20% glycerol, and 0.5 ml was loaded on top of a sucrose gradient (0.5 ml 53% sucrose, 1 ml 43% sucrose), and centrifuged for 2 h at 100,000 × *g*. Six 320-μL fractions were taken from the top, precipitated with an equal volume 20% trichloroacetic acid, and analyzed by SDS-PAGE gels and immunoblotting.

Live Imaging and Accumulation Quantification

Yeast cultures were grown to midlog phase in minimal media containing glucose, with the appropriate amino acids for selection. Cells were then washed once with water and once in galactose minimal media. Cells were then resuspended in galactose minimal media and plated onto PDL-coated glass-bottom dishes (MatTek, Ashland, MA). The minimal media was supplemented with Oxyrase (1:100, Oxyrase, Mansfield, OH) to minimize photodamage during fluorescence imaging. Warmed Oxyrase-containing medium, 1.5 ml, was added to the dish, and the lid was sealed with parafilm. The dish was then transferred on to a custom-built Plexiglas incubator housed over a Nikon TE-2000-E (Nikon, Tokyo, Japan) inverted epifluorescence microscope. The incubator was kept at ~30°C using an Air-Therm ATX temperature controller (World Precision Instruments, Sarasota, FL). To further minimize photodamage and photobleaching, the intensity of the fluorescence lamp was reduced to ~15% of total intensity using neutral-density filters. Under these conditions, yeast displayed normal growth and budding for the entire imaging session (10–16 h). Typically the exposure time was between 100 and 2000 ms, with the camera (CoolSnap-HQ, Photometrics, Tucson, AZ) operating at maximum gain. Images were typically captured at 60× or 100× magnification. All image acquisition and processing was done using Metamorph (Molecular Devices, Downingtown, PA). All images were scaled linearly in Metamorph and subsequently mounted in Adobe Photoshop (Adobe, San Jose, CA) for display.

Quantification of accumulations was done by capturing images of cultures that had been grown in galactose media for 16 h. Four fields from separate cultures were counted, with ~250 cells in each field, and cells were scored for presence of accumulations.

Electron Microscopy

Fixation was done by mixing equal volumes of cold 2× fixative and yeast cell suspensions, fixing for 5 min on ice, pelleting and resuspending in cold 1× fixative, and continuing fixation on ice for a total of 35 min. The final (1×) concentration of the fixative was 2% glutaraldehyde in 40 mM KPO_4 buffer, pH 6.7, 1 mM $MgCl_2$, 1 mM EGTA, and 1.0 M sorbitol. Cells were washed in decreasing concentrations of sorbitol in 40 mM KPO_4 buffer, washed 10 min in 50 mM NH_4Cl, and stored overnight in buffer. The next day, cells were treated for 10 min with freshly made 1% Na-m-periodate, rinsed in DH_2O, and washed for 10 min in 50 mM NH_4Cl. They were postfixed for 20–30 min in 0.5% OsO_4 + 0.8% K ferrocyanide in 0.1 M cacodylate buffer, pH 7.4, on ice, dehydrated in cold ethanol, embedded in LR White resin, and polymerized for 2 d at 45–47°C. Thin sections were stained for 10–20 min with bismuth subnitrate.

For immunostaining, thin sections were picked up on formvar-coated grids and immunostained floating on drops of solution. The buffer used was 10 mM tris-HCl in PBS + 0.02% NaH_3. The primary antibodies used were SNL1, a rabbit polyclonal antibody to α-syn and normal rabbit IgG. Antibody dilutions and blocking solution were spun for 5 min at 13,000 rpm on a microfuge before use. Sections were blocked for 45 min in 1% ovalbumin + 0.2% fish gelatin in buffer (block), incubated overnight at 4C in primary antibody in 1:10 dilution of block, washed five times for 5 min on buffer, blocked for 5 min, and incubated for 2.5–4 h on anti-rabbit IgG coupled to 10-nm colloidal gold in 1:10 block. They were washed three times with buffer, three times with dH_2O, dried, and stained for 10–20 min with bismuth subnitrate.

Electron microscopy was also conducted on samples of substantia nigra from a patient with PD that was harvested 2 h postmortem, fixed overnight in 4% paraformaldehyde and 0.1% glutaraldehyde, and cut into 50-μm sections with a Vibratome. The sections were fixed for an additional 10 min in 2% glutaraldehyde in 0.1 M cacodylate buffer, pH 7.4, postfixed for 30 min in 1% OsO_4 + 1.5% potassium ferrocyanide in buffer, dehydrated, and embedded in Epon.

Immunofluorescence

Cells were grown in galactose minimal media for 16 h and fixed in 4% paraformaldehyde in 40 mM phosphate buffer for 1 h at 30°C. Cells were then washed twice in 40 mM phosphate buffer containing 1.2 M sorbitol (sorbitol buffer) and incubated for 10 min at 30°C in sorbitol buffer containing 300 μg/ml zymolyase 100T (Seikagaku America, Rockville, MD) to digest the cell wall. Cells were then washed twice in sorbitol buffer and once in PBS containing 1% BSA, 0.5% Tween (Block buffer). Cells were then incubated with block buffer containing the appropriate dilution of primary antibody at 4°C overnight, washed twice in block buffer and incubated with secondary antibody for 1 h at room temperature. Cells were finally washed three times in block buffer and mounted on PDL-coated dishes for microscopy. Antibodies used for immunofluorescence were LB509, Syn303, and 12CA5, an anti-hemagglutinin (HA) antibody (Roche, Indianapolis, IN).

Genomic Red Fluorescent Protein Tagging

Endogenous proteins were red fluorescent protein (RFP) tagged as described (Sheff and Thorn, 2004). Briefly, sequence-specific primers were used to amplify mCherry RFP or dTomato dimeric RFP with the HISMX selection cassette and site-specific sequences for directed integration. These PCR products were used directly to transform yeast cells, which were then grown in selective media, and screened by fluorescence microscopy to confirm integration of the RFP tags.

Quantification of Sec7p and Cop1p disruption was measured in a blinded experiment by examining 10 fields from three different samples with ~100 cells per field. Sec7p disruption was first measured by examining the red channel. Cells with one or more discrete Sec7 punctate structures were considered normal, and cells with 0-labeled structures were considered disrupted. Cells containing large α-syn-EGFP accumulations were identified by examining the green channel. Cells with inclusions greater than or equal to 10% of the cell diameter were considered cells bearing large accumulations. These cells were then matched to the corresponding red channel image to examine Sec7p disruption.

Statistical Analysis

Comparison of sample means and calculation of P values was performed using GraphPad software (San Diego, CA).

RESULTS

α-Synuclein Accumulation in the Cytoplasm of S. cerevisiae Is Initiated at the Plasma Membrane

To gain insight into the sequence of events that lead to α-syn accumulation in the cytoplasm of *S. cerevisiae*, yeast strains expressing human WT and familial PD α-syn mutants with a C-terminal EGFP tag under control of a galactose-inducible, glucose-repressible promoter (α-syn-EGFP, A53T-EGFP and A30P-EGFP, respectively) were first examined in the 2μ pYES2 expression system and subsequently were integrated into the yeast genome upstream of the Gal1 promoter. Both integrated and nonintegrated α-syn constructs yielded similar results. Furthermore, a number of artificial α-syn mutants (Figure 1A) with N- or C-terminal truncations (denoted as 58-140-EGFP and 1-57-EGFP, respectively) as well as the fibrillization incompetent α-syn mutant, Δ71-82-EGFP (Giasson *et al.*, 2001) were also generated. The latter mutants were used in the structure-function studies described below.

To monitor expression of the various α-syn-EGFP constructs, immunoblot analysis was conducted using an anti-C-terminal–specific α-syn antibody (LB509), an anti-N-terminal antibody (Syn303), and an anti-EGFP antibody. All antibodies detected a major protein band with MW ~50 kDa and some minor breakdown products, suggesting the entire α-syn-EGFP fusion protein is expressed in the WT and mutant α-syn-EGFP cells (Figure 1B). An α-syn S129 phosphospecific antibody detected a phosphorylated isoform of α-syn-EGFP from cells expressing WT syn-EGFP, A53T-EGFP, A30P-EGFP, Δ71-82-EGFP, and 58-140-α-syn-EGFP (data not shown). α-Syn phosphorylation at S129 in yeast is unusual possibly because this site is not highly phosphorylated under physiological conditions (Okochi *et al.*, 2000), but it is heavily phosphorylated in LBs of PD and other synucleinopathies (Fujiwara *et al.*, 2002).

We also performed immunofluorescence using our anti-C (LB509) and anti-N (Syn303) terminal specific α-syn antibodies (Figure 1C) and showed that both antibodies completely colocalized with the EGFP fluorescence. As previously reported (Outeiro and Lindquist, 2003), untagged α-syn localized similar to EGFP-tagged α-syn in yeast (data not shown).

As shown previously (Outeiro and Lindquist, 2003; Zabrocki *et al.*, 2005; Dixon *et al.*, 2005), α-syn-EGFP prominently localized to plasma membranes and formed cytoplasmic accumulations, whereas EGFP alone showed a diffuse cytoplasmic distribution (Figures 1A and 2A). The α-syn clusters/accumulations varied considerably in size, and many of the smaller ones appeared to be associated with the cell cortex, whereas larger accumulations were sometimes completely localized to the cytoplasm, suggesting that they may form initially at the plasma membrane or the ER, which underlies the plasma membrane in yeast (Figure 1D). The binding of α-syn-GFP to plasma membrane was further confirmed biochemically in membrane fractionation studies. Although both α-syn-EGFP and EGFP were detected in the cytosolic fraction, a significant portion of α-syn-EGFP but not EGFP was recovered in the plasma membrane fractions (Supplementary Figure 1).

To determine the temporal sequence of the cytoplasmic accumulation of α-syn-EGFP, we performed live imaging studies on yeast cells expressing WT α-syn-EGFP. After induction with galactose, initial expression of the protein was observed at the cell cortex (Figure 1D). This was followed by the accumulation of small α-syn-EGFP aggregates at the cell cortex ~80 min later. Time-lapse microscopy demonstrated that the small accumulations grew in size and sometimes merged together to form larger accumulations that often appeared to detach from the cell cortex and assemble into cytoplasmic clusters (Figure 1D and Supplementary Information, Video 1 online). These experiments provide direct evidence indicating that membrane localization may be a required first step in the formation of α-syn accumulations in yeast cells.

α-Synuclein Accumulation in the Cytoplasm Requires Both the N-terminus and the NAC domain

Previous studies have shown that the N-terminal KTKEGV imperfect α-helical motifs are involved in membrane binding (Davidson *et al.*, 1998; Perrin *et al.*, 2000; Kim *et al.*, 2006), but it is unclear if they are required for α-syn localization to the plasma membrane. To test this possibility, we generated yeast cell lines expressing α-syn-EGFP fusion proteins with either the first 57 amino acids alone (1-57-EGFP) or with these residues deleted (58-140-EGFP; Figures 1A and 2A). Significantly, α-syn constructs with the N-terminus alone (1-57-EGFP) localized to the plasma membrane (Figure 2A), whereas α-syn constructs with an N-terminus deletion (58-140-EGFP) showed a diffuse cytoplasmic distribution with no membrane localization (Figures 2A and Supplementary Information, Video 2 online). A53T-EGFP, Δ71-82-EGFP, and β-syn-EGFP all localized to the membrane, consistent with the fact that these all contain the N-terminal α-helical repeats. Although A30P-EGFP was localized to the membrane, it did not form accumulations in the cytoplasm (Figures 2A and Supplementary Information, Video 3 online); this may be due to the substitution of alanine by a proline, a helix breaker, at the end of repeat 2. Consistent with this hypothesis, we observed substantial diffuse cytoplasmic A30P-EGFP, suggesting that this mutation may decrease membrane binding. However, an alternative explanation could be that A30P α-syn is specifically targeted to the

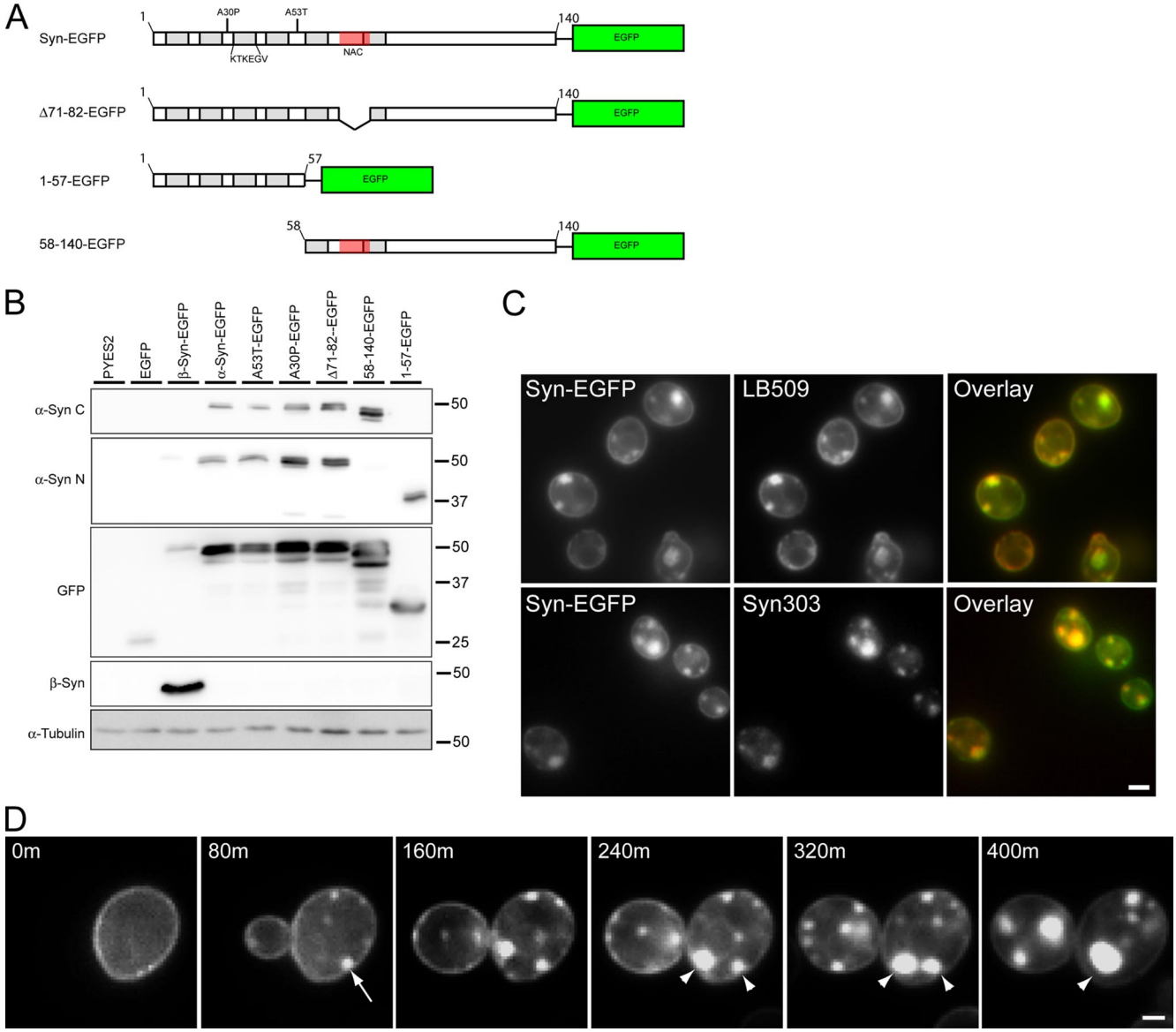

Figure 1. α-Syn-EGFP expression and accumulation in *S. cerevisiae.* (A) Schematic of α-syn-EGFP constructs used in this study. Locations of KTKEGV motif repeats, the hydrophobic residues 71-82 within the NAC domain, A30P and A53T point mutations, and truncated/deleted regions are indicated. (B) Immunoblot analysis of yeast extracts from cells expressing PYES2 constructs using a C-terminal anti-α-syn mAb (LB509), an N-terminal anti-α-syn mAb (Syn303), an anti-GFP antibody, an anti-β-syn mAb (Syn 207), and an α-tubulin antibody. (C) α-Syn immunofluorescence on yeast expressing α-syn-EGFP using LB509 and Syn303. Both mAb immunostaining colocalize completely with the GFP signal, indicating that the entire fusion protein is present. (D) Time-lapse imaging of α-syn-EGFP (PYES2 Syn-EGFP) accumulation formation in yeast. Images were taken every 80 min starting when syn-EGFP protein expression was visible. Membrane-associated accumulations begin to form at 80 min (arrow) and grow larger in size. Some accumulations appear to coalesce to form larger accumulations (arrowheads). For corresponding video, see Supplementary Information, Video1 online. Scale bars, (C) 2 μm; (D) 1 μm.

vacuole for degradation by the yeast protein YPP1 (Flowers *et al.*, 2007). Thus, our data demonstrated the requirement for the α-syn N-terminus and most likely the helical repeats therein for membrane localization.

The central hydrophobic NAC region of α-syn has been implicated as a crucial region for amyloid fibril formation and α-syn self-assembly (El Agnaf *et al.*, 1998; Giasson *et al.*, 2001). We determined if this region is also important for the formation of α-syn accumulations in this yeast model by generating yeast lines expressing a α-syn-EGFP fusion protein lacking amino acids 71-82 of α-syn (Δ71-82-EGFP, Figures 1A and 2A). Although Δ71-82-EGFP localized to the membrane at levels comparable to WT α-syn-EGFP, we observed a 10-fold decrease in the number of cells that developed α-syn accumulations (i.e., 2–3% in Δ71-82 vs. 30–35% in syn-EGFP cells, Figures 2B and Supplementary Information, Video 4 online). Furthermore, A53T-EGFP (which contains the entire NAC domain) but not β-syn-EGFP (which lacks residues 71-82) formed cytoplasmic accumulations. These results support an important role for residues 71-82 in mediating α-syn accumulation.

To evaluate whether or not membrane binding was sufficient to cause α-syn-EGFP accumulations, we compared the distribution of EGFP with the different syn-tagged EGFP fusion proteins 16 h after galactose induction. As expected, 1-57-EGFP was localized to the membrane, but there were

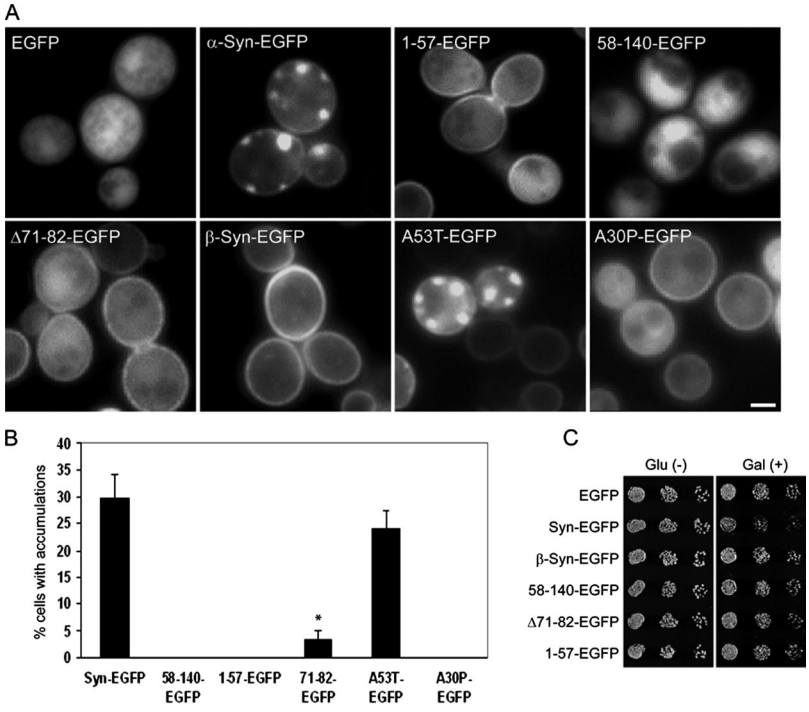

Figure 2. Structural requirements for α-syn-EGFP accumulation and toxicity in yeast. (A) Effect of deletions and mutations on α-syn-EGFP localization in yeast. EGFP alone has a diffuse localization, whereas WT α-syn-EGFP binds the plasma membrane and forms membrane associated accumulations. Deletion of the N-terminus (58-140-EGFP) eliminates membrane binding and α-syn accumulation, whereas expression of only the N-terminus (1-57-EGFP) preserves membrane binding but eliminates α-syn accumulation. The deletion of residues 71-82 (Δ71-82-EGFP), a region important for α-syn fibril formation, showed a dramatic reduction in the number of cells with α-syn accumulation although membrane localization is not impaired. Similarly, β-syn-EGFP also binds membrane but does not accumulate in the cytoplasm. A30P-EGFP shows membrane localization and cytoplasmic distribution but does not accumulate. (B) Quantification of the percentage of cells containing accumulations in yeast expressing different deletions and mutations of α-syn-EGFP. Error bars, SD. (C) Effect of various deletions on growth of yeast. Only cells expressing full-length α-syn have a growth defect. Scale bar, (A) 1 μm.

no accumulations (Figure 2A), suggesting that membrane binding alone is not sufficient to cause formation of accumulations. Similarly, although Δ71-82-EGFP was distributed to the membrane, only a small number of cytoplasmic α-syn clusters were detected. The N-terminal deletion, 58-140-EGFP, was not localized to the membrane and α-syn accumulations were not found. Thus, these data suggest that membrane binding is a necessary step for the formation of cytoplasmic accumulations of α-syn in yeast, but this step alone is not sufficient for accumulation to occur. Taken together, our time-lapse microscopy and structure-function experiments provide evidence that the accumulation of cytoplasmic α-syn occurs sequentially through a two-step process: The first step involves membrane binding, which probably requires the imperfect KTKEGV repeats at the N-terminus of α-syn, and the second step requires the hydrophobic NAC domain to drive accumulation of α-syn-EGFP.

Finally, to evaluate if the presence of α-syn accumulations results in toxicity (Outeiro and Lindquist, 2003, Cooper *et al.*, 2006), we performed growth assays to examine the effect of α-syn domain deletions on cell growth. As previously reported, α-syn-EGFP had a mild toxic effect on cell growth, and this effect was not observed with any of the α-syn deletion mutants or with β-syn, all of which did not form accumulations (Figure 2C). Our results support a role for α-syn accumulation in the inhibition of cell growth, because the elimination of these accumulations, either through elimination of membrane binding or deletion of the NAC region, abolishes this toxicity.

α-Syn-EGFP Accumulations Are Composed of Clusters of Vesicles in the Cytoplasm

To determine if α-syn-EGFP accumulations resemble PD-like LBs, we performed electron microscopy (EM) on the α-syn-EGFP accumulations. To facilitate imaging of these α-syn accumulations, we utilized cells with α-syn-EGFP integrated into the yeast genome. These cells produced twice the percentage of cytoplasmic α-syn accumulations as the nonintegrated strain (Supplementary Figure 2). The number of cells with α-syn accumulations was further enhanced to ~70% by treatment of these yeast with 5% DMSO (Zabrocki *et al.*, 2005). Surprisingly, EM analyses of the cells expressing α-syn-EGFP did not reveal filamentous α-syn- or LB-like structures. Instead, large accumulations of membranous vesicles, ranging in size from 20 to 100 nm in diameter were observed (Figure 3, A–C). These vesicular clusters were observed in cells expressing α-syn-EGFP and A53T-EGFP, but were not detected in cells expressing 1-57-EGFP, 58-140-EGFP, or EGFP alone, thereby indicating that these vesicular clusters are integral components of the α-syn accumulations visualized by fluorescence microscopy (Figure 3, compare panels A–C and G with panels D–F and H). Similar vesicular accumulations were also observed in cells grown without DMSO (Figure 3I), and in cells expressing untagged α-syn (Supplementary Figure 3).

To confirm that α-syn is indeed present within the vesicular clusters, immuno-EM was conducted using a polyclonal anti-α-syn antibody (SNL-1). Immunogold particles (localized α-syn) on or near vesicles within a cluster in α-syn-EGFP–expressing cells suggesting that α-syn is bound to the vesicles (Figure 3, J–L). As expected, plasma membrane localization of α-syn-EGFP immunogold particles was also evident (Figure 3, J–L). However, no plasma membrane localization or vesicular accumulations were detected in cells expressing 58-140-EGFP (Figure 3H). Elimination of the osmication resulted in more robust immunolabeling of α-syn in the plasma membrane and accumulations, but poorer preservation of organelle and vesicle structures (Figure 3L).

Our ultrastructural studies demonstrate that these α-syn-EGFP clusters are a collection of vesicular structures containing α-syn and are not α-syn amyloid fibrils that are the defining features of LBs in PD brains. This striking observation suggests a new mechanism for α-synuclein cellular toxicity that may be relevant to PD.

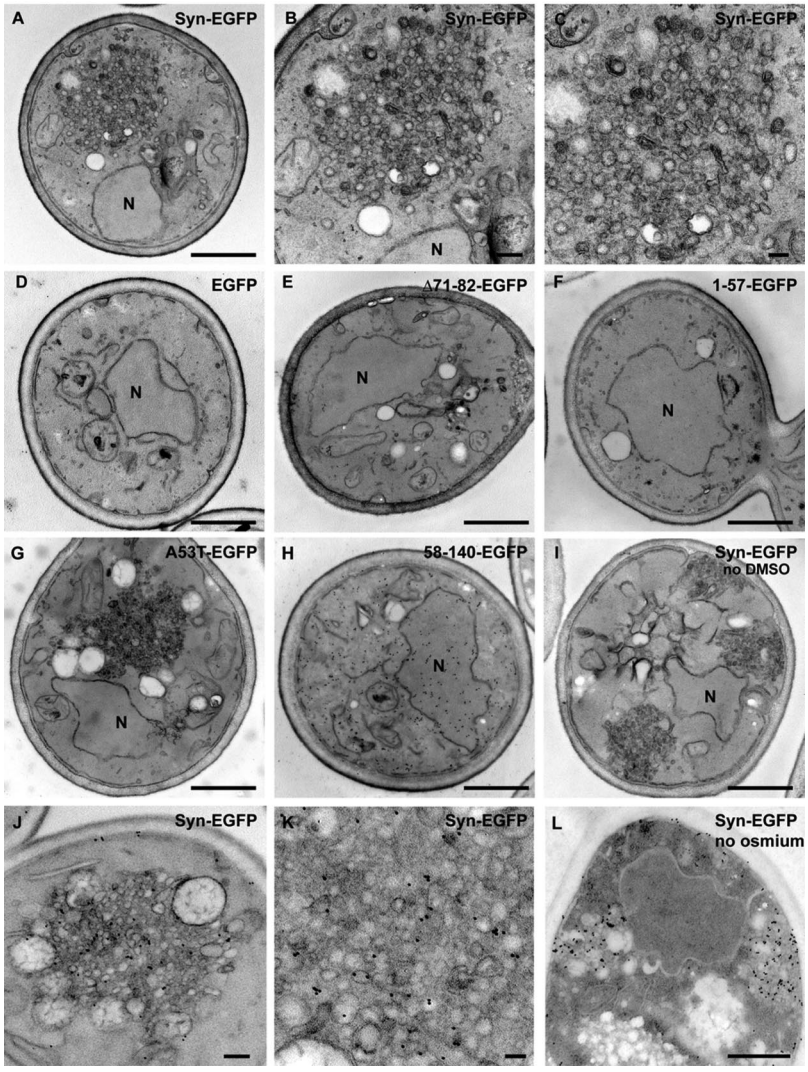

Figure 3. α-Syn-EGFP accumulations are composed of vesicles. Electron microscopy on yeast expressing α-syn-EGFP shows dense accumulations of vesicles (A–C), which do not appear in cells expressing EGFP alone (D). Cells expressing Δ71-82-EGFP (E), 1-57-EGFP (F), and 58-140-EGFP (H) do not have vesicular accumulations. Cells expressing A53T-EGFP have vesicular accumulations that are similar to wild type (G). Cells expressing α-synuclein without DMSO treatment formed similar accumulations (I). Immuno-EM using SNL-1, a polyclonal anti-α-syn antibody with 10-nm colloidal gold, shows that α-syn localizes to the vesicular accumulations (J–L), as well as the plasma membrane (J and L). Omission of osmication resulted in stronger antibody staining (L). Cells expressing EGFP alone had no staining with the anti-α-syn antibody (D), whereas cells expressing 58-140-EGFP displayed cytoplasmic staining (I). N, nucleus. Scale bars, (A, D–I, and L) 500 nm; (B and J) 100 nm; (C and K) 50 nm.

α-Syn Vesicular Clusters Contain Both Secretory Vesicles and ER-Golgi Transport Vesicles

To provide insights into the identity of the vesicles detected by EM, we evaluated the localization of HA-tagged Sec4p, a Rab GTPase which localizes to secretory vesicles (Guo *et al.*, 1999) and HA-tagged Ypt1p, a Rab GTPase involved in ER-Golgi transport that normally localizes to ER-Golgi transport vesicles (Morsomme and Riezman, 2002) with α-syn-EGFP. HA-tagged Sec4p colocalized with vesicular accumulations in cells expressing α-syn-EGFP (Figure 4A), whereas it had a diffuse granular localization in cells expressing EGFP alone. Similar to a recent study (Cooper *et al.*, 2006), α-syn-EGFP accumulations in yeast cells also colocalize with Ypt1p (Figure 4B). To demonstrate the specificities of HA-Sec4p and HA-Ypt1p in localizing to the correct vesicles, we examined the distribution of HA-tagged Vps29p, a peripheral membrane protein involved in endosome-to-Golgi retrograde transport (Seaman *et al.*, 1998), in EGFP and α-syn-EGFP expressing cells. Significantly, we found no difference in Vps29p localization (Figure 4C), indicating that the colocalization seen with HA-Sec4p and HA-Ypt1p is not an artifact of the HA tag itself. Thus, our experiments suggest that the α-syn accumulations are comprised of vesicles of multiple types, some of which contain secretory vesicle and ER-Golgi transport vesicle markers.

Vesicular Clustering Caused by α-Syn-EGFP Expression Disrupts Organization of the Golgi

To determine if the presence of large vesicular accumulations in cells expressing α-syn-EGFP disrupt the localization and function of other organelles, we examined the organization of the ER, Golgi, vacuole, and endosomes by genomically integrated RFP-tagged organelle markers in cells containing α-syn-EGFP vesicular accumulations. Using an RFP-tagged Sec63p, a protein involved in the translocation of polypeptides into the ER (Feldheim *et al.*, 1992), as a marker for yeast ER, we examined the localization of the ER in yeast cells expressing EGFP and α-syn-EGFP. A similar discontinuous distribution of Sec63p around the plasma membrane and also around the nucleus (Deshaies and Schekman, 1990) was observed in control and α-syn–expressing cells (Figure 5A), suggesting that the ER is not disrupted in cells with vesicular accumulations. The localization of the vacuole was also not disrupted by α-syn-EGFP accumulations, as shown in yeast cells expressing an RFP-tagged Vma4p (Figure 5B), a subunit of the vacuolar ATPase pump (Foury, 1990). The integrity of the endosomes is

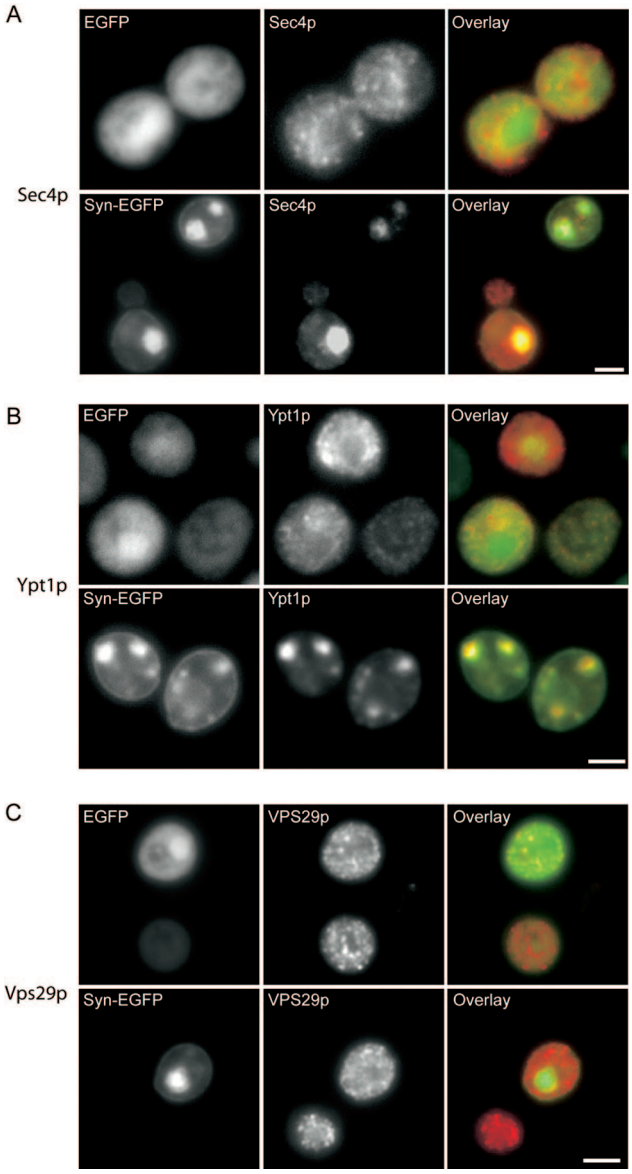

Figure 4. α-Syn-EGFP vesicular accumulations are colocalized with Rab GTPases Sec4p and Ypt1p. (A) α-Syn-EGFP accumulations are colocalized with Sec4p. 3HA-tagged-Sec4p was overexpressed (pRS413 3HA-Sec4p) in cells expressing either EGFP or α-syn-EGFP. In cells expressing EGFP or in α-syn-EGFP cells without accumulations, Sec4p was localized to small punctate structures throughout the cytoplasm (secretory vesicles). In cells with α-syn-EGFP accumulations, Sec4p staining was strongly colocalized with these accumulations. (B) α-Syn-EGFP accumulations are colocalized with Ypt1p. 3HA-tagged-Ypt1p was overexpressed (pRS413 3HA-Ypt1p) in cells expressing either EGFP or syn-EGFP. Cells were immunostained with anti-HA antibody. In cells expressing EGFP or α-syn-EGFP cells without accumulations, Ypt1p is localized to small punctate structures (most likely ER-Golgi transport vesicles) throughout the cytoplasm, whereas in cells with α-syn-EGFP accumulations, Ypt1p colocalizes with these accumulations. (C) 3HA-tagged-Vps29p did not colocalize with α-syn-EGFP accumulations, and localization of Vps29p was similar in cells expressing EGFP and α-syn-EGFP. Scale bar, 2 μm.

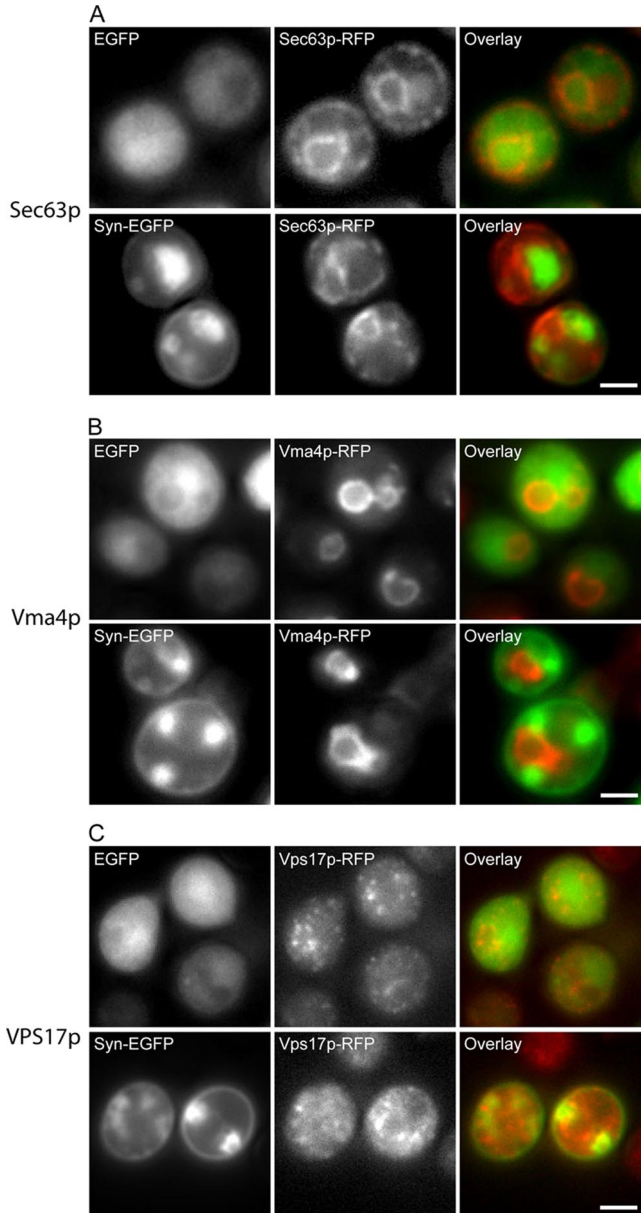

Figure 5. α-Syn-EGFP accumulations do not disrupt organization of the ER, vacuole, or Golgi. (A) Presence of α-syn-EGFP accumulations does not disrupt localization of the ER marker Sec63p. Sec63p was C-terminally tagged with monomeric RFP. Expression of EGFP or α-syn-EGFP shows similar localization of the ER marker. (B) Presence of α-syn-EGFP accumulations does not disrupt localization of the vacuole membrane marker Vma4p, which was c-terminally tagged with monomeric RFP. (C) Presence of α-syn-EGFP accumulations does not disrupt localization of the endosomal marker, Vps17p, which was c-terminally tagged with dimeric RFP. Scale bar, 2 μm.

also unaffected, because α-syn-EGFP expression in a strain of yeast with dimeric-RFP-tagged Vps17p (Figure 5C), a membrane protein involved in endosome-to-Golgi transport (Seaman *et al.*, 1998), did not cause any change in Vps17p distribution when compared with cells expressing EGFP alone.

To determine if α-syn-EGFP vesicular accumulations affect the organization of the Golgi, we examined the localization of RFP-tagged Sec7p, a guanine nucleotide exchange factor that localizes to late Golgi (Sata *et al.*, 1998). In cells expressing EGFP alone, Sec7p was localized to small punctate structures around the periphery of the cell. However, in cells containing α-syn-EGFP vesicular accumulations, the

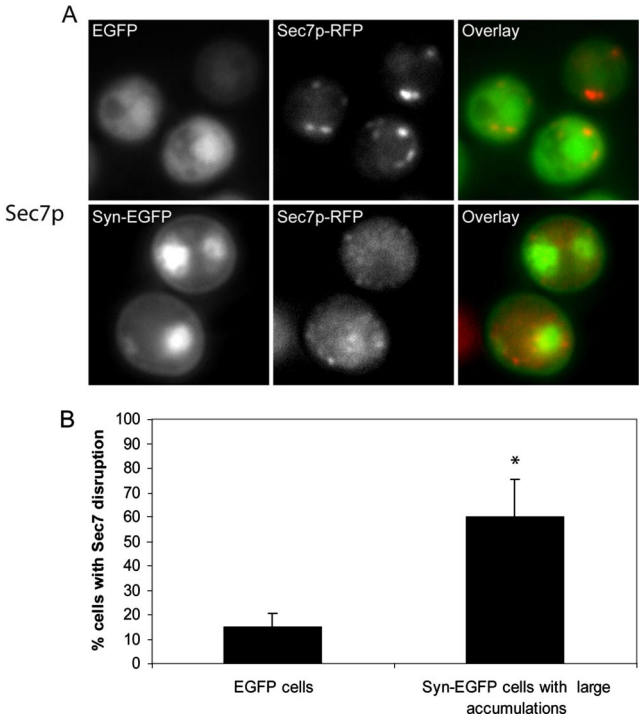

Figure 6. Presence of α-syn-EGFP accumulations disrupts localization of the Golgi marker Sec7p. (A) Presence of α-syn-EGFP accumulations disrupt localization of the late Golgi marker Sec7p, which was C-terminally tagged with monomeric RFP. Scale bar, 2 μm (B) Quantification of Sec7p disruption in cells expressing EGFP and cells expressing α-syn-EGFP with large accumulations. Scale bar, 2 μm.

Sec7p localization was disrupted, displaying a complete lack of discrete Sec7p puncta (Figure 6A). We quantified the disruption of Sec7p by comparing the localization of Sec7p in cells containing large (greater than or equal to 10% of the cell diameter) α-syn-EGFP accumulations with cells expressing EGFP alone. We found that there was a substantial increase ($p < 0.001$) in Sec7p disruption from cells expressing EGFP alone (14.8 ± 5.7%) to cells containing large α-syn-EGFP accumulations (60.1 ± 15.1%; Figure 6B). Cells expressing α-syn-EGFP without large accumulations displayed normal Sec7p localization, indicating that the formation of accumulations and not simple expression of α-syn is required for Sec7p disruption. A second Golgi marker, Cop1p, was examined and found to be disrupted in cells expressing Syn-EGFP compared with controls (Supplementary Figure 4, 67.2 ± 1.4% increase from control, $p < 0.0001$).

Taken together, these data show that α-syn vesicular accumulations in yeast results in a profound disruption of Golgi morphology, as indicated by Sec7p and Cop1p localization, but does not affect the localization of markers of ER, vacuole, or endosomes.

Evidence of Vesicular Accumulations in Human LBs

Our experiments thus far demonstrate that α-syn expression in yeast resulted in cytoplasmic accumulations of vesicles that are associated with toxicity. To determine if similar vesicular accumulations are found in LBs of PD, we examined the ultrastructure of LBs from the substantia nigra (from a 66-y-old PD patient) with a short postmortem interval and that was optimally fixed for EM. In this case, many typical LBs were observed (Figure 7, A–C). Additionally, we observed dense clusters of small vesicles around the perimeter of these LBs (Figure 7, A–E). These vesicles ranged in size between 20 and 100 nm. They were typically found around the edges of the LBs, away from the densely packed fibrils (Figure 7E). Examination of an area more distal to the LB revealed a lack of dense clusters of vesicles, although sparse vesicles that appear to be of similar size are visible (Figure 7F). These data are consistent with the earlier EM studies of LBs (Duffy and Tennyson, 1965) and suggest that vesicle accumulations, similar to those we report here in our yeast model system, may be important in the initial formation of LBs and the pathogenesis of PD.

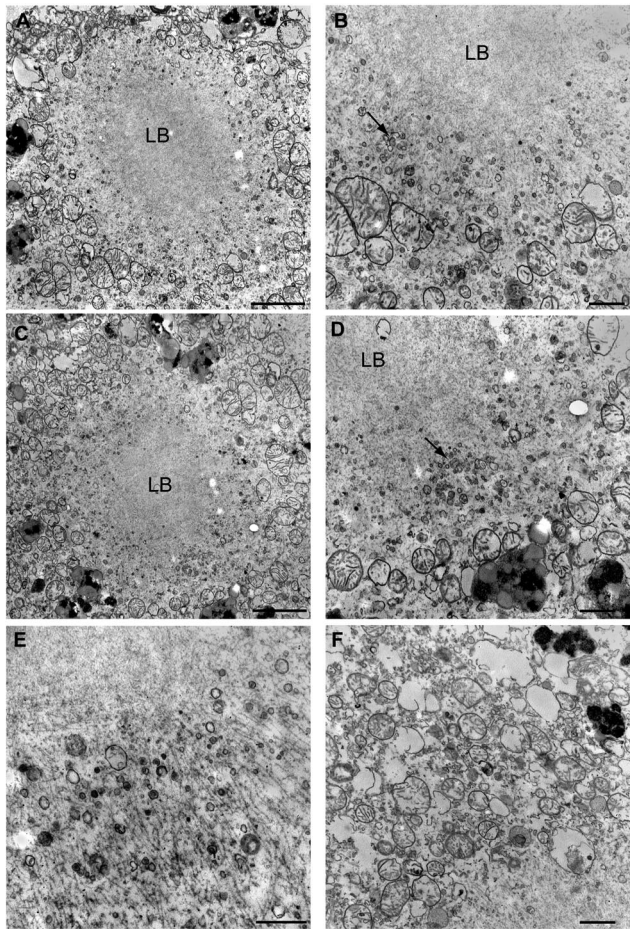

Figure 7. Presence of vesicular accumulations in human PD LBs. EM micrographs of LBs from the substantia nigra of a PD patient. LBs were composed of a dense fibrillar core with associated small vesicular accumulations (arrow) around the perimeter (A–E). Examination of sites more distal to the LBs revealed less dense distribution of small vesicles than that seen around the LB perimeter (F). Scale bars, (A, C, and E) 2 μm. (B, D, and F) 500 nm.

DISCUSSION

Here, we have examined the process of α-syn-EGFP accumulation in yeast. We have demonstrated that α-syn accumulation requires an intact N-terminus as well as the NAC domain and that clustered vesicles are integral components of α-syn accumulations similar to those observed in authentic LBs in PD. The consequences of these α-syn accumulations in yeast include the disruption of the Golgi, as well as the disruption of ER-to-Golgi and secretory vesicular trafficking, and cellular toxicity. Importantly, the overexpres-

sion of α-syn in yeast cells did not produce LB-like filamentous α-syn amyloid structures, but did recruit the accumulation of vesicles as in PD LBs. Although not a direct model for recapitulating insoluble inclusions containing amyloid α-syn, this model may provide insights into the potential function of α-syn and/or the early steps in the formation of LBs because similar vesicular accumulations are detected in human LBs of PD.

On induction with galactose, α-Syn-EGFP was first localized to the cell cortex. This interaction with membranes appears to be dependent upon the N-terminal α-helical repeats of α-syn, because deletion of this subdomain abrogates this early membrane localization. This is consistent with previous studies demonstrating that these N-terminal repeats bind phospholipids and lipid membranes and may be critical for the normal function of α-syn (Perrin *et al.*, 2000; Kim *et al.*, 2006) and that mutations in this region perturbs plasma membrane localization in yeast (Volles and Lansbury, 2007). Hence, we propose that the binding of α-syn to the yeast plasma membrane may mimic its ability to bind synaptic vesicles in neurons and may be a useful system to study the membrane-binding function of α-syn. Furthermore, we show here that membrane localization of α-syn is required for the subsequent recruitment of vesicles, because the deletion of N-terminal repeats eliminated this membrane localization as well as vesicular clustering.

However, our data also support the view that membrane localization alone is insufficient to cause vesicle clustering because expressing the first 57 amino acids of α-syn is sufficient to cause membrane localization, but not vesicle accumulation. We also determined that deletion of the hydrophobic residues 71-82 within the NAC domain greatly reduced the ability of α-syn to induce vesicular clustering in yeast, without affecting membrane localization. Thus, the formation of vesicular accumulations may depend on the ability of α-syn to form intermolecular interactions through the hydrophobic NAC domain. Alternatively, this region may be important for α-syn to assume a conformation change that facilitates vesicle interaction.

Our EM studies revealed that α-syn-EGFP accumulations are composed of collections of vesicles. These vesicular clusters do not contain fibrils, unlike authentic human LBs. However, alterations in synaptic vesicle numbers due to manipulation of α-syn levels have been reported, including evidence that suppression of α-syn expression in cultured neurons reduced of the distal pool of synaptic vesicles (Murphy *et al.*, 2000), that α-syn knockout mice demonstrate an impairment in the maintenance of the reserve pool of synaptic vesicles (Cabin *et al.*, 2002), and that overexpression of α-syn in PC12 cells results in an accumulation of "docked" vesicles at the synapse (Larsen *et al.*, 2006). α-Syn–induced accumulation of vesicles in yeast may mimic the ability of α-syn to regulate synaptic vesicles in neurons. Therefore, *S. cerevisiae* may be a useful system for studying the role of α-syn in the regulation and maintenance of synaptic vesicle pools.

The presence of α-syn–induced vesicular accumulations caused a severe disruption of the organization of the Golgi apparatus, but did not disrupt the ER, vacuole, or endosomes. A previous study showed that expression of α-syn caused disruption of ER-Golgi transport and cytotoxicity (Cooper *et al.*, 2006), whereas our data suggest that disruption of the Golgi organization may contribute to this phenotype. Golgi fragmentation has been observed in nigral neurons with α-syn–positive LBs, particularly in neurons containing pale bodies that are thought to represent an early stage of LBs formation (Fujita *et al.*, 2006), suggesting that the Golgi fragmentation caused by α-syn expression in yeast may be relevant to abnormalities in the human disease. Golgi fragmentation has also been observed as a consequence of prefibrillar α-syn aggregates in cell culture (Gosavi *et al.*, 2002). These two observations, in addition to our data, suggest that α-syn could contribute to toxicity even when it is not in a fibrillar state and that these vesicular accumulations may represent early stages of LB formation as well as PD pathogenesis. Thus, the formation of similar vesicular accumulations in neurons could serve as a concentration point or scaffold for the formation of α-syn filaments and subsequent LB formation.

One interesting observation in this yeast system is that the familial α-syn mutations, A30P and A53T, do not enhance vesicular accumulation. In fact, A30P α-syn does not form vesicular accumulations in yeast. Currently, it is unclear how A30P causes familial PD. The impaired binding to rat brain vesicles (Jensen *et al.*, 1998) and in yeast cells suggest that it could lead to a reduction in α-syn transport to presynaptic terminals and a loss of function in the asymmetric neuron. On the other hand, A53T α-syn was shown to enhance fibrillization in both test tube studies and in transgenic mouse models of synucleionopathies when compared with WT α-syn (Conway *et al.*, 1998, Giasson *et al.*, 1999, 2002). Thus, the lack of increased vesicle clustering in yeast cells expressing the A53T mutant suggests that this mutation does not cause disease by increasing vesicular accumulation. A previous report (Cooper *et al.*, 2006) showed that the A53T mutation caused a CPY trafficking block in yeast at earlier time points than WT α-synuclein. However, there was no reported difference in toxicity between WT and A53T α-synuclein expressing cells, suggesting that this CPY trafficking defect may be independent of vesicular accumulation and toxicity. Alternatively, the difference in CPY trafficking between WT and A53T α-synuclein may be insufficient to cause changes in the size and the number of vesicle clusters. Because α-syn fibrils are not detected in α-syn–expressing yeast cells, our data are consistent with enhanced fibril formation due to the A53T mutation being downstream from vesicle accumulations. Finally, these yeast models of synucleinopathies may represent unique systems to study α-syn disruption of cellular trafficking and toxicity in PD that is independent from α-syn fibril formation.

Although ER-Golgi transport-vesicle markers accumulate in yeast based on the colocalization of α-syn-EGFP with Ypt1 (Cooper *et al.*, 2006), our EM data suggest that there may be several other types of vesicles in the α-syn-EGFP vesicular inclusions, because vesicles of various sizes are observed. For example, we identified Sec4p, a secretory vesicle associated Rab GTPase within α-syn-EGFP accumulations, suggesting that secretory vesicles are also present. Thus, our data suggest that the α-syn-EGFP accumulations include vesicular accumulations composed of at least two different types of vesicles in the transport and secretion pathway and that α-syn is able to disrupt vesicular organization at two stages of the transport/secretion pathway. However, it cannot be ruled out that the markers themselves are mislocalized and that these are not true secretory transport vesicles. This observation may reflect an exaggeration of the normal function of α-syn, which has been hypothesized to play a role in the organization and recycling of synaptic vesicles. When α-syn is overexpressed or misregulated in humans, it may disrupt these pathways. However, in yeast there are no synaptic vesicles and α-syn may perform similar functions involving other types of vesicles, including secretory vesicles and ER-Golgi transport vesicles.

α-syn–induced vesicular accumulations, as demonstrated here in yeast, may represent an important early step in the pathogenesis of PD. Indeed, dense accumulations of vesicles concentrated in the periphery of LBs were observed in neurons in the substantia nigra of a PD patient. These vesicles may be the remains of larger vesicular accumulations that were caused by vesicle binding of α-syn as seen in the yeast model. These vesicular structures may provide a scaffold for α-syn fibrillization and therefore may be directly involved in the formation of pathological LBs. Although examination of additional cases is required to verify these findings, vesicular accumulations have been observed in neuronal pale body-like structures that have been speculated to be precursors of LBs (Hayashida *et al.*, 1993). Thus, accumulation of α-syn–associated vesicles may result in the eventual formation of fibrillar α-syn as LBs, which compromise neuronal survival. Alternatively, the accumulation of vesicles may directly result in neuronal toxicity. Further examination of cell and animal models is needed to explore these hypotheses.

In conclusion, we have demonstrated that the inclusions seen in *S. cerevisiae* expressing α-syn are comprised of clusters of vesicles. Although vesicular accumulations can be detected in LB-containing neurons in human PD, α-syn amyloid fibrils are present in authentic LBs but not in yeast cells, suggesting that vesicular clustering may be an early step in the pathogenesis of LB. Future studies in this and other model systems will provide additional insight into the exact relationship between this vesicular accumulation phenotype and α-syn fibril formation in human neurodegenerative diseases.

ACKNOWLEDGMENTS

We thank Dr. Kelvin Luk for his critical reading of our manuscript and Dr. Hiro Uryu (University of Pennsylvania) for providing the human PD case material. This work was supported by grants from the National Institutes of Health (AG-P01-09215, GM T32 07229) and the Picower Foundation. V.M.-Y.L. is the John H. Ware III professor in Alzheimer's disease research. J.Q.T. is the William Maul Measey-Truman G. Schnabel, Jr. Chair of Geriatric Medicine and Gerontology. We acknowledge the Penn Bio-Imaging Core for electron microscopy, and we thank the families of the patients used in this study.

REFERENCES

Abeliovich, A. *et al.* (2000). Mice lacking alpha-synuclein display functional deficits in the nigrostriatal dopamine system. Neuron *25*, 239–252.

Cabin, D. E. *et al.* (2002). Synaptic vesicle depletion correlates with attenuated synaptic responses to prolonged repetitive stimulation in mice lacking alpha-synuclein. J. Neurosci. *22*, 8797–8807.

Chandra, S., Gallardo, G., Fernandez-Chacon, R., Schluter, O. M., and Sudhof, T .C. (2005). Alpha-synuclein cooperates with CSPalpha in preventing neurodegeneration. Cell *123*, 383–396.

Chartier-Harlin, M. C. *et al.* (2004). Alpha-synuclein locus duplication as a cause of familial Parkinson's disease. Lancet *364*, 1167–1169.

Cole, N. B., Murphy, D. D., Grider, T., Rueter, S., Brasaemle, D., and Nussbaum, R. L. (2002). Lipid droplet binding and oligomerization properties of the Parkinson's disease protein alpha-synuclein. J. Biol. Chem. *277*, 6344–6352.

Conway, K. A., Harper, J. D., and Lansbury, P. T. (1998). Accelerated in vitro fibril formation by a mutant alpha-synuclein linked to early-onset Parkinson disease. Nat. Med. *4*, 1318–1320.

Cooper, A. A. *et al.* (2006). α-Synuclein blocks ER-Golgi traffic and Rab1 rescues neuron loss in Parkinson's models. Science *313*, 324–328.

Davidson, W. S., Jonas, A., Clayton, D. F., and George, J. M. (1998). Stabilization of alpha-synuclein secondary structure upon binding to synthetic membranes. J. Biol. Chem. *273*, 9443–9449.

Deshaies, R. J., and Schekman, R. (1990). Structural and functional dissection of Sec62P, a membrane-bound component of the yeast endoplasmic-reticulum protein import machinery. Mol. Cell. Biol. *10*, 6024–6035.

Dixon, C., Mathias, N., Zweig, R. M., Davis, D. A., and Gross, D. S. (2005). Alpha-synuclein targets the plasma membrane via the secretory pathway and induces toxicity in yeast. Genetics *170*, 47–59.

Duda, J. E., Lee, V. M.-Y., and Trojanowski, J. Q. (2000). Neuropathology of synuclein aggregates. J. Neurosci. Res. *61*, 121–127.

Duda, J. E., Giasson, B. I., Mabon, M. E., Lee, V. M.-Y., Trojanowski, J. Q. (2002). Novel antibodies to synuclein show abundant striatal pathology in Lewy body diseases. Ann. Neurol. *52*, 205–210.

Duffy, P. E., and Tennyson, V. M.-Y. (1965). Phase and electron microscopic observations of Lewy bodies and melanin granules in substantia nigra and locus caeruleus in Parkinsons disease. J. Neuropathol. Exp. Neurol. *24*, 398–407.

El Agnaf, O. M., Jakes, R., Curran, M. D., Middleton, D., Ingenito, R., Bianchi, E., Pessi, A., Neill, D., and Wallace, A. (1998). Aggregates from mutant and wild-type alpha-synuclein proteins and NAC peptide induce apoptotic cell death in human neuroblastoma cells by formation of beta-sheet and amyloid-like filaments. FEBS Lett. *440*, 71–75.

Feldheim, D., Rothblatt, J., and Schekman, R. (1992). Topology and functional domains of Sec63P, an endoplasmic-reticulum membrane-protein required for secretory protein translocation. Mol. Cell. Biol. *12*, 3288–3296.

Flower, T. R., Chesnokova, L. S., Froelich, C. A., Dixon, C., and Witt, S. N. (2005). Heat shock prevents alpha-synuclein-induced apoptosis in a yeast model of Parkinson's disease. J. Mol. Biol. *351*, 1081–1100.

Flower, T. R., Clark-Dixon, C., Metoyer, C., Yang, H., Shi, R., Zhang, Z., Witt, S. N. (2007). YGR198w (YPP1) targets A30P alpha-synuclein to the vacuole for degradation. Journal of Cell Biology *177*, 1091–1104.

Forman, M. S., Lee, V. M.-Y., and Trojanowski, J. Q. (2005). Nosology of Parkinson's disease: looking for the way out of a quagmire. Neuron *47*, 479–482.

Foury, F. (1990). The 31-kDa polypeptide is an essential subunit of the vacuolar ATPase in *Saccharomyces cerevisiae.* J. Biol. Chem. *265*, 18554–18560.

Fujita, Y., Ohama, E., Takatama, M., Al Sarraj, S., and Okamoto, K. (2006). Fragmentation of Golgi apparatus of nigral neurons with alpha-synuclein-positive inclusions in patients with Parkinson's disease. Acta Neuropathol. *112*, 261–265.

Fujiwara, H., Hasegawa, M., Dohmae, N., Kawashima, A., Masliah, E., Goldberg, M. S., Shen, J., Takio, K., and Iwatsubo, T. (2002). alpha-Synuclein is phosphorylated in synucleinopathy lesions. Nat. Cell Biol. *4*, 160–164.

Galvin, J. E., Lee, V. M.-Y., and Trojanowski, J. Q. (2001). Synucleinopathies: clinical and pathological implications. Arch. Neurol. *58*, 186–190.

George, J. M., Jin, H., Woods, W. S., and Clayton, D. F. (1995). Characterization of a novel protein regulated during the critical period for song learning in the zebra finch. Neuron *15*, 361–372.

Giasson, B. I., Jakes, R., Goedert, M., Duda, J. E., Leight, S., Trojanowski, J. Q., and Lee, V. M.-Y. (2000). A panel of epitope-specific antibodies detects protein domains distributed throughout human alpha-synuclein in Lewy bodies of Parkinson's disease. J. Neurosci. Res. *59*, 528–533.

Giasson, B. I., Duda, J. E., Quinn, S. M., Zhang, B., Trojanowski, J. Q., Lee, V. M.-Y. (2002). Neuronal alpha-synucleinopathy with severe movement disorder in mice expressing A53T human alpha-synuclein. Neuron *34*, 521–533.

Giasson, B. I., Murray, I. V., Trojanowski, J. Q., and Lee, V. M.-Y. (2001). A hydrophobic stretch of 12 amino acid residues in the middle of alpha-synuclein is essential for filament assembly. J. Biol. Chem. *276*, 2380–2386.

Giasson, B. I., Uryu, K., Trojanowski, J. Q., and Lee, V. M.-Y. (1999). Mutant and wild type human alpha-synucleins assemble into elongated filaments with distinct morphologies in vitro. J. Biol. Chem. *274*, 7619–7622.

Gietz, D., Stjean, A., Woods, R. A., and Schiestl, R. H. (1992). Improved method for high-efficiency transformation of intact yeast-cells. Nucleic Acids Res. *20*, 1425.

Gosavi, N., Lee, H. J., Lee, J. S., Patel, S., and Lee, S. J. (2002). Golgi fragmentation occurs in the cells with prefibrillar alpha-synuclein aggregates and precedes the formation of fibrillar inclusion. J. Biol. Chem. *277*, 48984–48992.

Greenbaum, E. A., Graves, C. L., Mishizen-Eberz, A. J., Lupoli, M. A., Lynch, D. R., Englander, S. W., Axelsen, P. H., and Giasson, B. I. (2005). The E46K mutation in alpha-synuclein increases amyloid fibril formation. J. Biol. Chem. *280*, 7800–7807.

Guo, W., Roth, D., Walch-Solimena, C., and Novick, P. (1999). The exocyst is an effector for Sec4p, targeting secretory vesicles to sites of exocytosis. EMBO J. *18*, 1071–1080.

Han, H., Weinreb, P. H., and Lansbury, P. T., Jr. (1995). The core Alzheimer's peptide NAC forms amyloid fibrils which seed and are seeded by beta-

amyloid: is NAC a common trigger or target in neurodegenerative disease? Chem. Biol. *2*, 163–169.

Hayashida, K., Oyanagi, S., Mizutani, Y., and Yokochi, M. (1993). An early cytoplasmic change before Lewy body maturation—an ultrastructural-study of the substantia-nigra from an autopsy case of juvenile parkinsonism. Acta Neuropathol. *85*, 445–448.

Iwai, A., Masliah, E., Yoshimoto, M., Ge, N., Flanagan, L., de Silva, H. A., Kittel, A., and Saitoh, T. (1995). The precursor protein of non-A beta component of Alzheimer's disease amyloid is a presynaptic protein of the central nervous system. Neuron *14*, 467–475.

Jakes, R., Crowther, R. A., Lee, V. M.-Y., Trojanowski, J. Q., Iwatsubo, T., Goedert, M. (1999). Epitope mapping of LB509, a monoclonal antibody directed against human alpha-synuclein. Neurosci. Lett. *269*, 13–16.

Jensen, P. H., Nielsen, M. S., Jakes, R., Dotti, C. G., and Goedert, M. (1998). Binding of alpha-synuclein to brain vesicles is abolished by familial Parkinson's disease mutation. J. Biol. Chem. *273*, 26292–26294.

Juschke, C., Ferring, D., Jansen, R. P., and Seedorf, M. (2004). A novel transport pathway for a yeast plasma membrane protein encoded by a localized mRNA. Curr. Biol. *14*, 406–411.

Kim, Y. S., Laurine, E., Woods, W., and Lee, S. J. (2006). A novel mechanism of interaction between alpha-synuclein and biological membranes. J. Mol. Biol. *360*(2), 386–397.

Kruger, R., Kuhn, W., Muller, T., Woitalla, D., Graeber, M., Kosel, S., Przuntek, H., Epplen, J. T., Schols, L., and Riess, O. (1998). Ala30Pro mutation in the gene encoding alpha-synuclein in Parkinson's disease. Nat. Genet. *18*, 106–108.

Kushnirov, V. V. (2000). Rapid and reliable protein extraction from yeast. Yeast *16*, 857–860.

Larsen, K E. *et al*. (2006). Alpha-synuclein overexpression in PC12 and chromaffin cells impairs catecholamine release by interfering with a late step in exocytosis. J. Neurosci. *46*, 11915–11922.

Maroteaux, L., Campanelli, J. T., and Scheller, R. H. (1988). Synuclein: a neuron-specific protein localized to the nucleus and presynaptic nerve terminal. J. Neurosci. *8*, 2804–2815.

Maroteaux, L., and Scheller, R. H. (1991). The rat brain synucleins; family of proteins transiently associated with neuronal membrane. Brain Res. Mol. Brain Res. *11*, 335–343.

Morsomme, P., and Riezman, H. (2002). The Rab GTPase Ypt1p and tethering factors couple protein sorting at the ER to vesicle targeting to the Golgi apparatus. Dev. Cell *2*, 307–317.

Murphy, D. D., Rueter, S. M., Trojanowski, J. Q., and Lee, V. M.-Y. (2000). Synucleins are developmentally expressed, and alpha-synuclein regulates the size of the presynaptic vesicular pool in primary hippocampal neurons. J. Neurosci. *20*, 3214–3220.

Okochi, M., Walter, J., Koyama, A., Nakajo, S., Baba, M., Iwatsubo, T., Meijer, L., Kahle, P. J., and Haass, C. (2000). Constitutive phosphorylation of the Parkinson's disease associated alpha-synuclein. J. Biol. Chem. *275*, 390–397.

Outeiro, T. F., and Lindquist, S. (2003). Yeast cells provide insight into alpha-synuclein biology and pathobiology. Science *302*, 1772–1775.

Perrin, R. J., Woods, W. S., Clayton, D. F., and George, J. M. (2000). Interaction of human alpha-Synuclein and Parkinson's disease variants with phospholipids. Structural analysis using site-directed mutagenesis. J. Biol. Chem. *275*, 34393–34398.

Polymeropoulos, M. H. *et al.* (1997). Mutation in the alpha-synuclein gene identified in families with Parkinson's disease. Science *276*, 2045–2047.

Sata, M., Donaldson, J. G., Moss, J., and Vaughan, M. (1998). Brefeldin A-inhibited guanine nucleotide-exchange activity of Sec7 domain from yeast Sec7 with yeast and mammalian ADP ribosylation factors. Proc. Natl. Acad. Sci. USA *95*, 4204–4208.

Seaman, M.N.J., McCaffery, J. M., and Emr, S. D. (1998). A membrane coat complex essential for endosome-to-Golgi retrograde transport in yeast. J. Cell Biol. *142*, 665–681.

Sheff, M. A., and Thorn, K. S. (2004). Optimized cassettes for fluorescent protein tagging in *Saccharomyces cerevisiae*. Yeast *21*, 661–670.

Singleton, A. B. *et al.* (2003). alpha-Synuclein locus triplication causes Parkinson's disease. Science *302*, 841.

Spillantini, M. G., Crowther, R. A., Jakes, R., Hasegawa, M., and Goedert, M. (1998). alpha-Synuclein in filamentous inclusions of Lewy bodies from Parkinson's disease and dementia with lewy bodies. Proc. Natl. Acad. Sci. USA *95*, 6469–6473.

Spillantini, M. G., Schmidt, M. L., Lee, V. M.-Y., Trojanowski, J. Q., Jakes, R., and Goedert, M. (1997). Alpha-synuclein in Lewy bodies. Nature *388*, 839–840.

Volles, M. J., and Lansbury, P. T., Jr. (2007). Relationships between the sequence of alpha-synuclein and its membrane affinity, fibrillization propensity, and yeast toxicity. J. Mol. Biol. *366*, 1510–1522.

Weinreb, P. H., Zhen, W., Poon, A. W., Conway, K. A., and Lansbury, P. T., Jr. (1996). NACP, a protein implicated in Alzheimer's disease and learning, is natively unfolded. Biochemistry *35*, 13709–13715.

Zabrocki, P., Pellens, K., Vanhelmont, T., Vandebroek, T., Griffioen, G., Wera, S., van Leuven, F., and Winderickx, J. (2005). Characterization of alpha-synuclein aggregation and synergistic toxicity with protein tau in yeast. FEBS J. *272*, 1386–1400.

Zarranz, J. J. *et al.* (2004). The new mutation, E46K, of alpha-synuclein causes Parkinson and Lewy body dementia. Ann. Neurol. *55*, 164–173.